SECA-TR-92-06

ADAPTION OF MULTIDIMENSIONAL GROUP PARTICLE TRACKING AND PARTICLE WALL-BOUNDARY CONDITION MODEL TO THE FDNS CODE

Subcontract 91-177
Contract No. NAS8-36955
Final Report

Prepared by:

Y. S. Chen
R. C. Farmer

Prepared for:

University of Alabama in Huntsville
Huntsville, AL 35899

March, 1992

SECA, Inc.
3313 Bob Wallace Avenue
Suite 202
Huntsville, AL 35805

Table of Contents

Introduction

A particulate two-phase flow CFD model was developed based on the FDNS code (Refs. 1,2,3) which is a pressure based predictor plus multi-corrector Navier-Stokes flow solver. Turbulence models with compressibility correction (Ref.4) and the wall function models (Ref. 5) were employed as submodels. A finite-rate chemistry model (Refs. 6,7) was used for reacting flow simulation. For particulate two-phase flow simulations, a Eulerian-Lagrangian solution method using an efficient implicit particle trajectory integration scheme was developed in this study. Effects of particle-gas reaction and particle size change to agglomeration or fragmentation were not considered in this investigation.

At the onset of the present study, a two-dimensional version of FDNS which had been modified to treat Lagrangian tracking of particles (FDNS-2DEL) had already been written and was operational. The FDNS-2DEL code was too slow for practical use, mainly because it had not been written in a form amenable to vectorization on the Cray, nor was the full three-dimensional form of FDNS utilized. The specific objective of this study was to reorder the calculations into long single arrays for automatic vectorization on the Cray and to implement the full three-dimensional version of FDNS to produce the FDNS-3DEL code. Since the FDNS-2DEL code was slow, a very limited number of test cases had been run with it. This study was also intended to increase to number of cases simulated to verify and improve, as necessary, the particle tracking methodology coded in FDNS.

Governing Equation

The gas-phase governing equations of the FDNS module are the

Reynolds-averaged Navier-Stokes equations with the addition of particle drag forces and heat fluxes in the momentum equations and the energy equation, respectively. Due to the effect of large density differences between the particles and the surrounding gas, the drag force was considered to be the primary contribution to the inter-phase momentum exchange. The gas-phase governing equations are written as:

$$J^{-1}(\partial \rho q/\partial t) = \partial[-\rho U_i q + \mu_{eff} G_{ij}(\partial q/\partial \xi_j)]/\partial \xi_i + S_q$$

where q = 1, u, v, w, h, k, ϵ and α_i for the continuity, momentum, energy, turbulence model and chemical species transport equations respectively. And, the transformation parameters and effective viscosity, μ_{eff}, are given as:

$$J = \partial(\xi,\eta,\zeta)/\partial(x,y,z)$$
$$U_i = (u_j/J)(\partial \xi_i/\partial x_j)$$
$$G_{ij} = (\partial \xi_i/\partial x_k)(\partial \xi_j/\partial x_k)/J$$
$$\mu_{eff} = (\mu + \mu_t)/\sigma_q$$

The source terms in the governing equations, S_q, are given as:

$$S_q = J^{-1}\begin{bmatrix} 0 \\ -p_x + \nabla[\mu_{eff}(u_j)_x] - (2/3)(\mu_{eff}\nabla u)_x + Dx \\ -p_y + \nabla[\mu_{eff}(u_j)_y] - (2/3)(\mu_{eff}\nabla u)_y + Dy \\ -p_z + \nabla[\mu_{eff}(u_j)_z] - (2/3)(\mu_{eff}\nabla u)_z + Dz \\ Dp/Dt + h_v + H_p - u_p\,Dx - v_p\,Dy - w_p\,Dz \\ \rho(P_r - \epsilon) \\ \rho(\epsilon/k)[(C_1 + C_3 P_r/\epsilon)\,P_r - C_2\epsilon] \\ \omega_n \end{bmatrix}$$

where Dx, Dy and Dz represent the drag forces and n takes on

values between 1 and N. u_p, v_p and w_p are the particle velocity components. H_p is the rate of heat transfer per unit volume to the gas phase. h_v stands for the viscous heat flux of the gas phase. P_r stands for the turbulence kinetic energy production rate and is written as:

$$P_r = (\mu_t/\rho)\,[(\partial u_j/\partial x_i + \partial u_i/\partial x_j)^2/2 - 2(\partial u_k/\partial x_k)^2/3]$$

An equation of state, $\rho = p/(RT/M_w)$, is used to close the above system of equations. Turbulent Schmidt and Prandtl numbers, σ_q, for the governing equations and other turbulence model constants are given taken from Refs. 4, 6 and 7.

Finite Rate Chemistry Model

For gas-phase chemical reaction modeling, a general system of chemical reactions is written in terms of the stoichiometric coefficients (ν_{ij} and ν_{ij}') and the i-th chemical species name (M_i) of the j-th reaction as

$$\sum_i \nu_{ij}\, M_i = \sum_i \nu_{ij}'\, M_i'$$

The net rate of change in the molar concentration of species i due to reactions j , X_{ij}, is written as:

$$X_{ij} = (\nu_{ij}'-\nu_{ij})\;[K_{fj}\Pi(\rho\alpha_i/M_{wi})^{\nu ij} - K_{bj}\Pi(\rho\alpha_i/M_{wi})^{\nu ij'}]$$

and the species production rate, ω_i, (in terms of mass fraction) is calculated by summing over all reactions.

$$\omega_i = M_{wi}\,\Sigma_j X_{ij}$$

where

M_{wi} = molecular weight of species i

α_i = mass fraction of species i

ρ = fluid density

K_{fj} = forward rate of reaction j

K_{bj} = backward rate of reaction j = K_{fj}/K_{ej}

K_{ej} = equilibrium constant

$= (1/RT)^{\Sigma(\nu ij' - \nu ij)} \exp(\Sigma(f_i'\nu_{ij}' - f_i\nu_{ij}))$

f_i = Gibbs free energy of species i

$K_f = A\ T^B \exp(-E/RT)$

Finally, the species continuity equations are written as:

$$\rho\ D_t\alpha_i - \nabla[(\mu_{eff}/\sigma_\alpha)\nabla\alpha_i] = \omega_i$$

where σ_α (assumed to be 0.9) represents the Schmidt number for turbulent diffusion. A penalty function is employed to ensure the basic element conservation constraints at the end of every time marching step. This is a crucial requirement for the numerical stability and accuracy of a CFD combustion model. This is accomplished by limiting the allowable changes in species concentrations, which are the solutions of the species continuity equations, for each time step such that the species mass fractions are well bounded within physical limits. The resulting limited changes are adjusted so that they are proportional to the species source terms. A similar chemistry approach and detailed turbulence submodels were reported previously (Ref. 8).

Particulate-Phase Equations

A Eulerian-Lagrangian particle tracking method was employed in FDNS to provide effects of momentum and energy exchanges between the gas phase and the particle phase. The particle

trajectories are calculated using an efficient implicit time integration method for several groups of particle sizes by which the drag forces and heat fluxes are then coupled with the gas phase equations. The equations constitute the particle trajectory and temperature history are written as:

$$DV_i/Dt = (U_i - V_i)/t_d$$
$$Dh_p/Dt = C_{pc} (T_{aw} - T_p)/t_H - 6 \sigma \epsilon f T_p^4/(\rho_p d_p)$$

where U_i = Gas Velocity
V_i = Particle Velocity
t_d = Particle Dynamic Relaxation Time
= $4 \rho_p d_p/(3 C_d \rho_c |U_i - V_i|)$
h_p = Particle Enthalpy
C_{pc} = Particle Heat Capacity
T_p = Particle Temperature
T_{aw} = Gas Recovery Temperature
t_H = Particle Thermal-Equilibrium Time
= $(\rho_p d_p)/[12 Nu \mu/(Pr d_p)]$
σ = Stefan-Boltzmann Constant
= 4.76E-13 BTU/FT^2-S-R
ϵ = Particle Emissivity = 0.20 -- 0.31
f = Radiation Interchange Factor
d_p = Particle Diameter
ρ_p = Particle Density

C_d and Nu stand for drag coefficient and Nusselt number for heat transfer which are functions of Reynolds number and relative Mach number. Typical correlations are given in Refs. 9 and 10. Carlson and Hoglund's correlation (Ref. 9) is written as:

$$C_d = (24/Re)\ (1 + 0.15\ Re^{0.687})\ (1 + e^{-a})/ [1 + M\ (3.82 + 1.28\ e^{-1.25Re/M})/Re]$$

$$Nu = (1 + 0.2295\ Re^{0.55})/ [1 + 3.42\ M\ (2 + 0.459\ Re^{0.55})/Re]$$

where $a = 0.427/M^{4.63} + 3.0/Re^{0.88}$. A more accurate but more complicated correlation for the drag coefficient is provided by Henderson (Ref. 10). That is, for Mach ≥ 1,

$$C_d = 24\ [Re + S\ \{4.33 + \exp(-0.247\ Re/S)\ (3.65 - 1.53\ T_w/T) /(1 + 0.353\ T_w/T)\}]^{-1} + \exp(-0.5*M/Re^{1/2})[0.1M^2 + 0.2M^8 + (4.5 + 0.38a) /(1 + a)] + 0.6\ S\ [1 - \exp(-M/Re)]$$

where $S = M(\gamma/2)^{1.2}$ is the molecular speed ratio. $a = 0.03\ Re + 0.48\ Re^{1/2}$. For Mach ≥ 1.75,

$$C_d = [0.9 + 0.34/M^2 + 1.86(M/Re)^{1/2}\ \{2 + 2/S^2 + 1.058\ (T_w/T)^{1/2}/S - 1/S^4\}]\ /\ [1 + 1.86\ (M/Re)^{1/2}]$$

And, for 1 < Mach < 1.75,

$$C_d = C_{d\ M=1} + (4/3)\ (M - 1)\ (C_{d\ M=1.75} - C_{d\ M=1})$$

which assumes a linear variation between M = 1 and M = 1.75.

It has been shown that the Henderson drag law gives better motor performance predictions compared with test data. The applicability and possible improvement of the Nusselt number correlation is currently being actively researched (Ref. 11).

Details of the Particle Solution Method

In the present two-phase flow model, an independent module was employed for the calculation of particle drag forces and heat flux contributions to the gas flow field. Subroutines for locating the particles and integrating their trajectories are called for each particle size group. The drag forces and heat fluxes are then saved for every grid point. These forces and fluxes are then used to evaluate the particle source terms in the gas-phase governing equations. In the present FDNS flow solver, two forms of the energy equation (i.e. static enthalpy form or total enthalpy form) can be selected. It has been found that although either form of energy equation usually gives similar solutions, the static enthalpy equation provides better definition of the liquid rocket plume shear layers, as shown by extensive solutions made for the SSME. A determination of which form the energy equation best simulates solid (two-phase) rocket motor plumes has not yet been made.

Particle wall-boundary conditions are treated by using a specified fraction of the colliding particles which stick to the wall. Particles which stick result in a decreased particle velocity normal to the wall for that particle size fraction. Therefore, for the particle size fraction which locally collides with the wall, part of the particles stick and the other part is turned more parallel to the wall. Energy exchange is assumed to be due only to the particles which stick. This model of particle wall interaction can be improved, but new experimental test data must become available in order to do so.

In the 2-D version of the FDNS flow solver, a fourth-order Runge-Kutta method was employed to integrate the particle trajectories. After a thorough test of the integration routine,

it was found that the explicit scheme can sometimes give diverged particle solutions when the source terms become large. Therefore, an implicit integration scheme was employed in the present model. For convenience, consider the X-component of the particle equation of motion. That is,

$$dX_p/dt = U_p$$
$$dU_p/dt = A\ (U_c - U_p)$$

where $A = 1/t_d$
U_c = gas velocity
U_p = particle velocity
X_p = particle location

In finite difference form the above equations can be written as:

$$X_p^{(n+1)} - X_p^{(n)} = (\Delta t/2)\ [U_p^{(n+1)} + U_p^{(n)}]$$
$$U_p^{(n+1)} - U_p^{(n)} = \Delta tA\ [U_c - U_p^{(n+1)}]$$

or

$$X_p^{(n+1)} = X_p^{(n)} + \Delta t/2\ [U_p^{(n+1)} + U_p^{(n)}]$$
$$U_p^{(n+1)} = [U_p^{(n)} + \Delta tA\ U_c]/(1+\Delta tA)$$

These two equations are unconditionally stable despite the magnitude of the source terms. To provide better time resolution, a variable time step size is chosen so that a particle would take at least 4 time steps to go across a grid cell.

The recognition that an improved integration scheme was needed for calculating the particle trajectories was a major hurdle in developing FDNS-3DEL. The explicit scheme appeared to give acceptable solutions, but detailed comparisons to previous FDNS-2DEL analyses showed that unacceptable pressure losses were

predicted. Several other factors were initially suspected of causing this solution behavior. Namely, the turbulence model, the form of the energy equation, and the particle drag law were initially suspected, and lengthy calculations were made before these effects were found not to be the cause of poor results. Since the FDNS-2DEL results were found to give good pressure field comparisons to conventional nozzle and plume flowfield codes (RAMP, SPP, and SPF-II), the Runge-Kutta method was not expected to perform poorly in the FDNS-EL code. Resolving this problem consumed much of the resources which otherwise would have been used to run a wider variety of test cases.

Test Cases

The major test case which was studied was the Tomahawk solid rocket motor nozzle analysis. Consideration of a plume flowfield and of an oxygen-hydrogen coaxial injector was also made. These cases are described in the following paragraphs.

- The Tomahawk Nozzle Flowfield

The Tomahawk nozzle flowfield was calculated with FDNS-3DEL and is shown in Figs. 1-4. This test case was chosen because comparable predictions with the FDNS-2DEL and RAMP codes had already been performed, and these other solutions were available for comparison (Ref. 12). Figures 1-4 show the velocity, Mach number, temperature, and water concentration profiles, respectively, for the chamber, nozzle, and near plume. The chamber flow was approximated to be uniform so that direct comparisons with the previous solutions could be made. The FDNS-2DEL solution predicted somewhat lower exit plane centerline gas temperatures (2250 °K) than the RAMP solution (2400 °K). The FDNS-3DEL (2470 °K) and RAMP solutions show essentially the same exit plane centerline gas temperatures. The raggedness in the temperature profile near the centerline in the nozzle appears to be due to a weak oblique shock. An apparent non-zero temperature normal gradient at the centerline in the subsonic portion of the nozzle flowfield is indicated. This is due to a very strong effect of the inlet particle flowfield boundary condition. In a complete SRM simulation which includes the burning grain, more particles would flow down the centerline from the chamber (as compared to the uniform flow case) and this subsonic temperature contour would probably change shape. The sharp breaks in the velocity, Mach number, and temperature contours locate the approximate limiting streamline of the particle laded flow with

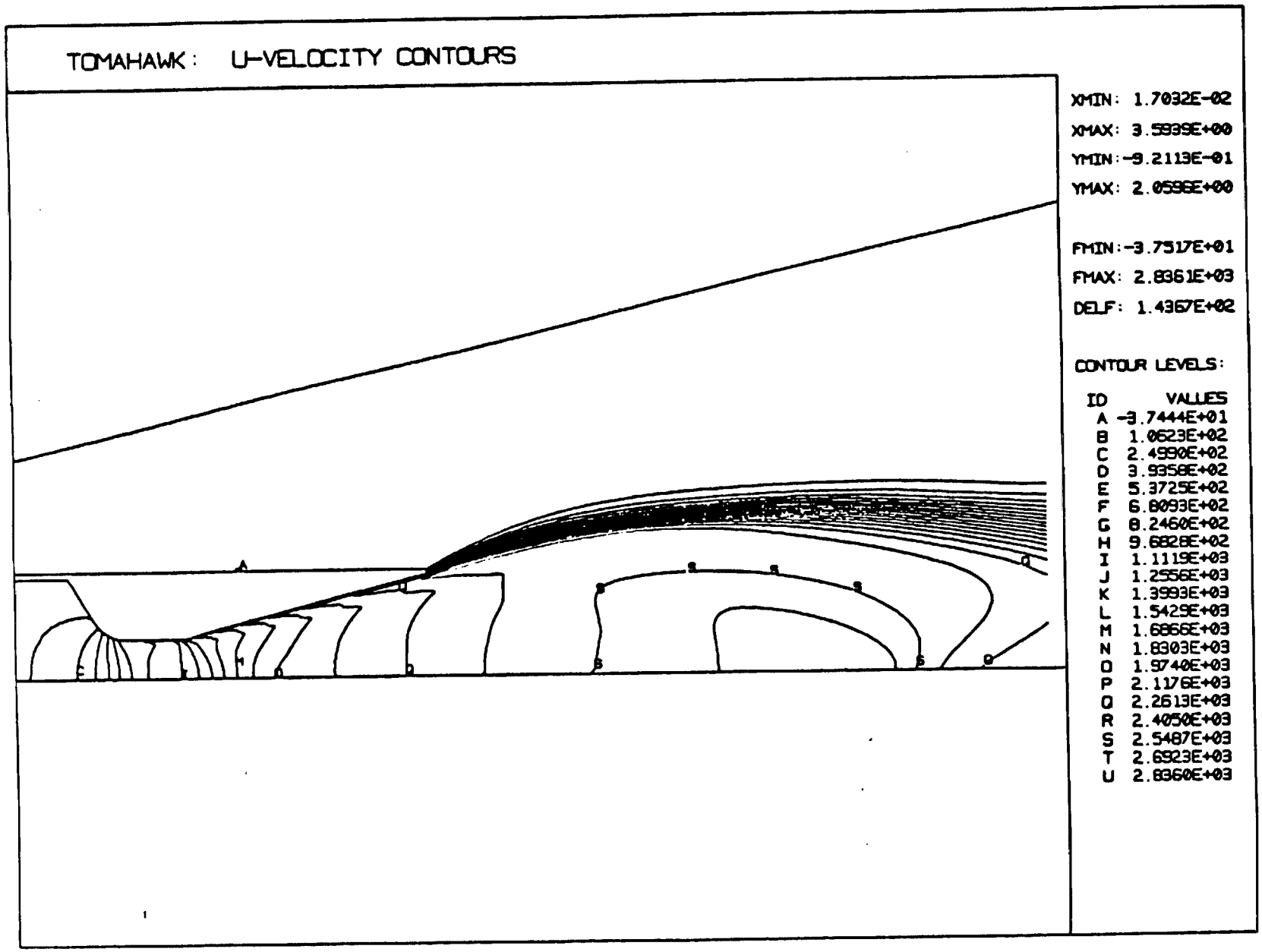
TOMAHAWK: U-VELOCITY CONTOURS
XMIN: 1.7032E-02
XMAX: 3.5939E+00
YMIN: -9.2113E-01
YMAX: 2.0596E+00
FMIN: -3.7517E+01
FMAX: 2.8361E+03
DELF: 1.4367E+02
CONTOUR LEVELS:
ID VALUES
A -3.7444E+01
B 1.0623E+02
C 2.4990E+02
D 3.9358E+02
E 5.3725E+02
F 6.8093E+02
G 8.2460E+02
H 9.6828E+02
I 1.1119E+03
J 1.2556E+03
K 1.3993E+03
L 1.5429E+03
M 1.6866E+03
N 1.8303E+03
O 1.9740E+03
P 2.1176E+03
Q 2.2613E+03
R 2.4050E+03
S 2.5487E+03
T 2.6923E+03
U 2.8360E+03

Figure 1

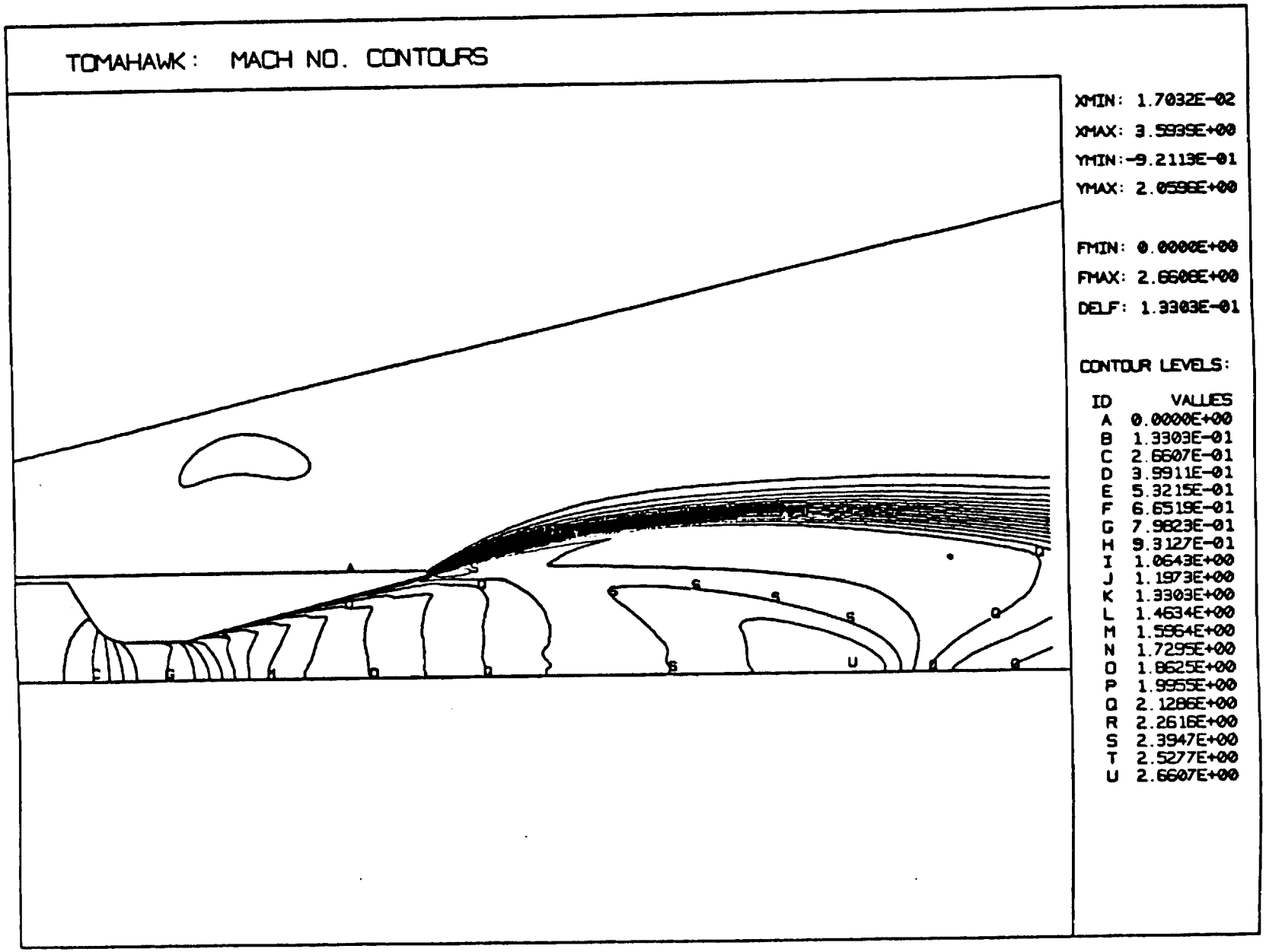
TOMAHAWK: MACH NO. CONTOURS
XMIN: 1.7032E-02
XMAX: 3.5939E+00
YMIN: -9.2113E-01
YMAX: 2.0598E+00
FMIN: 0.0000E+00
FMAX: 2.6608E+00
DELF: 1.3303E-01
CONTOUR LEVELS:
ID VALUES
A 0.0000E+00
B 1.3303E-01
C 2.6607E-01
D 3.9911E-01
E 5.3215E-01
F 6.6519E-01
G 7.9823E-01
H 9.3127E-01
I 1.0643E+00
J 1.1973E+00
K 1.3303E+00
L 1.4634E+00
M 1.5964E+00
N 1.7295E+00
O 1.8625E+00
P 1.9955E+00
Q 2.1286E+00
R 2.2616E+00
S 2.3947E+00
T 2.5277E+00
U 2.6607E+00

Figure 2

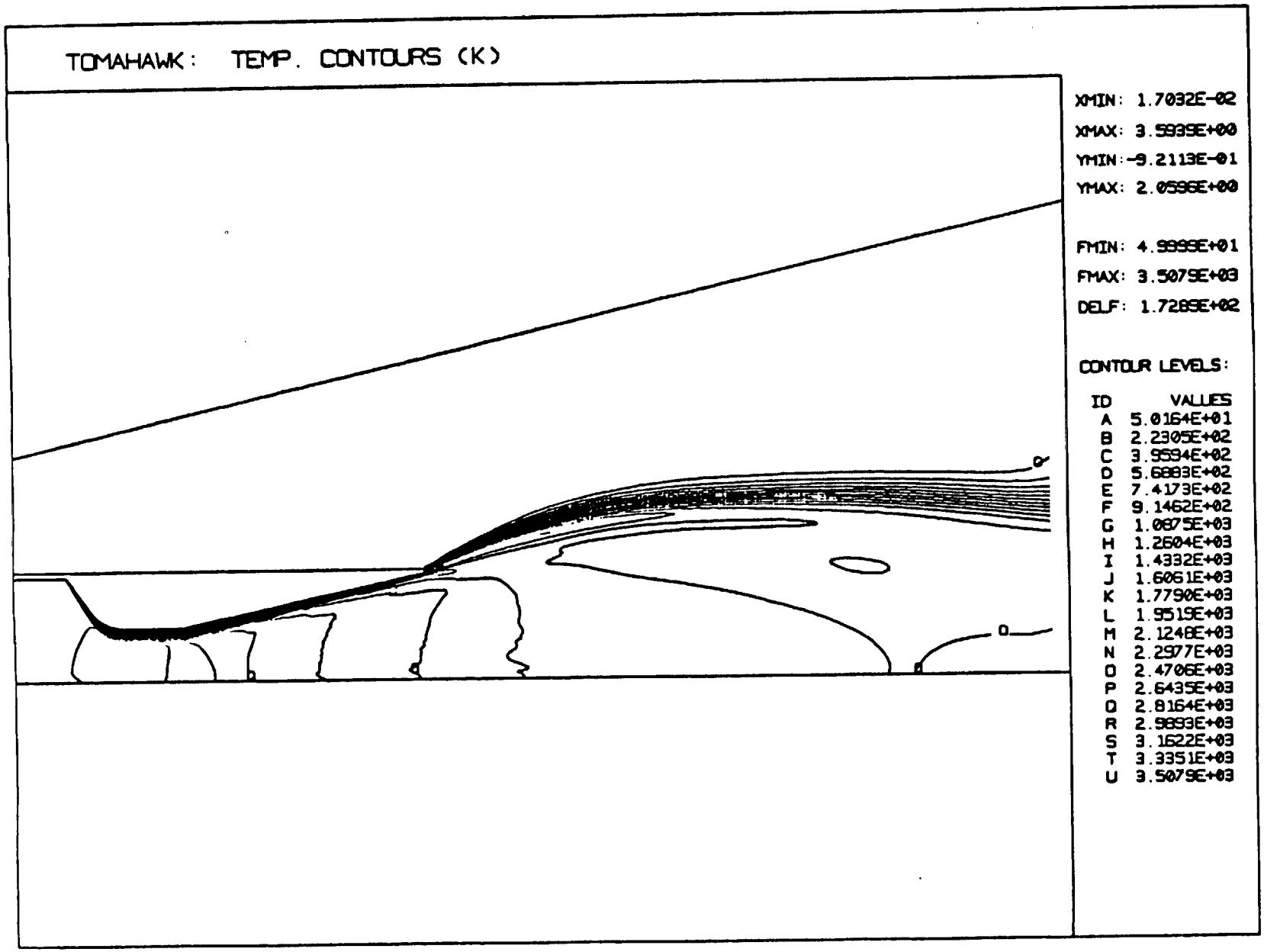
TOMAHAWK: TEMP. CONTOURS (K)
XMIN: 1.7032E-02
XMAX: 3.5939E+00
YMIN: -9.2113E-01
YMAX: 2.0596E+00
FMIN: 4.9999E+01
FMAX: 3.5079E+03
DELF: 1.7289E+02
CONTOUR LEVELS:
ID VALUES
A 5.0164E+01
B 2.2305E+02
C 3.9594E+02
D 5.6883E+02
E 7.4173E+02
F 9.1462E+02
G 1.0875E+03
H 1.2604E+03
I 1.4332E+03
J 1.6061E+03
K 1.7790E+03
L 1.9519E+03
M 2.1248E+03
N 2.2977E+03
O 2.4706E+03
P 2.6435E+03
Q 2.8164E+03
R 2.9893E+03
S 3.1622E+03
T 3.3351E+03
U 3.5079E+03

Figure 3

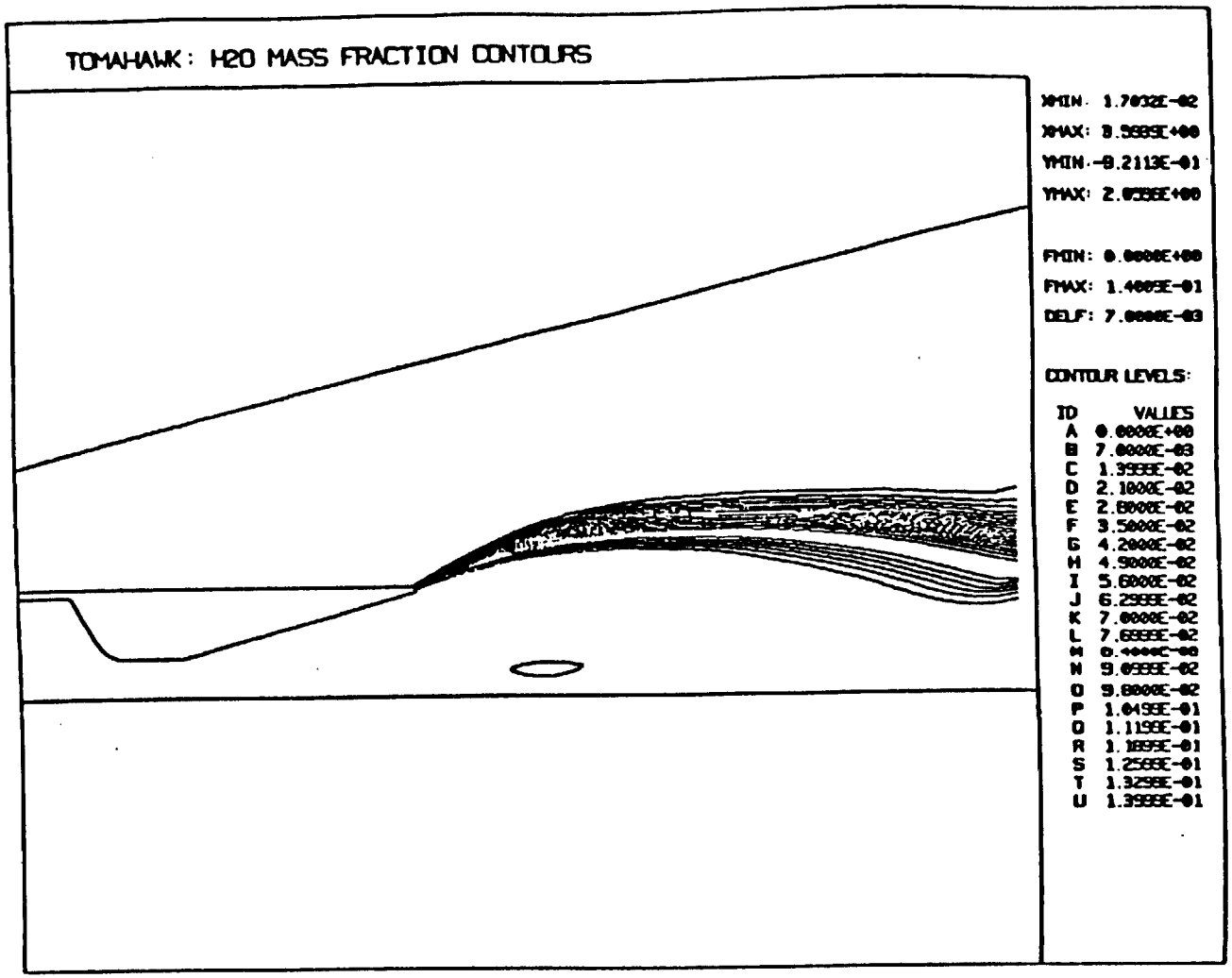
TOMAHAWK: H2O MASS FRACTION CONTOURS
XMIN: 1.7032E-02
XMAX: 8.5885E+00
YMIN:-8.2113E-01
YMAX: 2.0288E+00
FMIN: 0.0000E+00
FMAX: 1.4005E-01
DELF: 7.0000E-03
CONTOUR LEVELS:
ID VALUES
A 0.0000E+00
B 7.0000E-03
C 1.3988E-02
D 2.1000E-02
E 2.8000E-02
F 3.5000E-02
G 4.2000E-02
H 4.9000E-02
I 5.6000E-02
J 6.2988E-02
K 7.0000E-02
L 7.6888E-02
M 8.4000E-02
N 9.0988E-02
O 9.8000E-02
P 1.0498E-01
Q 1.1198E-01
R 1.1898E-01
S 1.2598E-01
T 1.3298E-01
U 1.3998E-01

Figure 4

respect to gas only flow which fills the nozzle. Both the static and total enthalpy forms of the energy equation give the same nozzle solutions. Letting the particles which hit the wall stick or elastically reflect give well behaved solutions. The only place where there is significant particle impact on the wall is at the start of the converging section. The analysis allows particles which hit the plume centerline to spectrally reflect, in order to account for particles crossing the plume centerline. However, particle drag moves the particles very parallel to the gas streamlines in the transonic region of the nozzle, such that such reflection does not occur in the case being considered.

- The Tomahawk Plume Flowfield

The near plume appears to be well predicted with FDNS-3DEL. The predicted free shear layer is sharply defined and indicates water production from afterburning reactions. Both the static and total form of the energy equation were considered. The total form of the energy equation indicates a temperature spike at the inception of the free shear layer. Better definition of the induced flow on the outside of the nozzle would probably eliminate such a spike. The static form of the energy equation does not exhibit this effect. A Mach number correction to the $k-\epsilon$ turbulence model was used for this simulation.

When the Tomahawk plume is calculated for a long distance down stream of the exit plane with FDNS-2DEL, excessively rapid plume/atmosphere mixing is predicted. This was believed to be due to the effect of crossing the Mach disc in the plume and thereby creating too much turbulent kinetic energy with the $k-\epsilon$ turbulence model being used. A similar problem exists when using the SPF/II standard JANNAF plume code (Ref. 13). The remedy in the SPF/II code is to switch turbulence models between the near

and far plumes. An insufficient number of test cases have been run with FDNS-3DEL to determine if the Mach number modified turbulence model will indeed fix this problem, although the solution is better behaved than when the extended k-ϵ turbulence model is used. This potential plume prediction problem for far-field analysis must be left for future resolution. The FDNS-3DEL code should not require any change other than turbulence model parameters to adjust the rate of plume/atmosphere mixing. It should be noted that the computed results with FDNS-2DEL, at first glance, look like the afterburning combustion reaction rates are too slow. Actually, so much of the cold atmosphere had mixed with the plume that the existence of afterburning was not apparent.

- Liquid Injector Flowfields

The current version of FDNS-3DEL does not treat mass transport from the particle phase to the gas (or continuous) phase. Also, the particle phase is treated with a lumped model such that the particle temperature is constant throughout the particle at any instant of time during the flow through the computation field. These restrictions should be removed before the code is useful for describing spray combustion. However, the spread of a droplet cloud of supercritical fuel or LOX could be described with the code without modification, if one is content with not describing local mixture ratio changes, i.e. one assumes that the supercritical lump remains a lump (or particle) in the region of the flow being analyzed. The energy transfer for supercritical injection could be easily treated in this manner because the heat of vaporization does not have to be considered. In fact, models which are based on arbitrarily supplying such heat of vaporization (Ref. 14), do not realistically describe supercritical spray phenomena. The only reason that such models

work at all is that the heat of vaporization evaluated at the temperature of the oxygen lump crudely approximates the high heat capacity of the liquid-like lump at supercritical pressures. An oxygen spray eminating from a single coaxial injector could be described with FDNS-3DEL by assuming the oxygen lump to be of a constant size and density. A demonstration calculation of this nature was considered, but the lump density would be such a very strong function of the mean lump temperature that the calculation was not performed. If accurate real-gas equation of state models were used, the stated oxygen spray simulation would be meaningful. Currently, SECA is developing the more general property evaluation for a hydrogen-oxygen engine heat transfer analysis (Ref. 15). However, the currently feasible constant property analysis was not made, because a reliable two-phase, 3-dimensional FDNS-3DEL code was not completed early enough in this study.

Closure

The calculation of two-phase reacting flows at best is a slow process. Several strategies were tried to make this process more efficient. Initially, ideal gas flow was computed, then the reactions were turned on, and finally the particle trajectories were calculated. The entire flowfield was calculated for each of these flow conditions. Recently, all of these conditions have been treated simultaneously from the beginning of the analysis. This procedure works well and results in an overall reduction in computation time. For analyzing rocket motors and their attendant plumes, it is recommended that the flowfield should be broken into subregions for analysis, in order to use the optimum step size for the Mach number range within the region. Such a restart option has been incorporated in FDNS-3DEL. For example, the motor and nozzle should be analyzed first. The computed

nozzle exit conditions should be used to calculate the near plume. The far plume should then be computed. The break between the near and far plume should be chosen somewhere between the establishment of the complex near field shock structure and the essentially balanced jet, predominately mixing dominated far field. The development of a parabolized version FDNS-3DEL to initially predict large plume structures and other large flowfields is also recommended.

Conclusions

1. A two-phase, finite-rate CFD code (FDNS-3DEL) was developed and vectorized. The Tomahawk nozzle test case indicates the CFD solution accurately simulates this flow.

2. Particle mass transfer effects are not currently included in the current code. The inclusion of these effects would be relatively simple.

3. More test cases should be run to establish the range of validity of the calculation procedure. The mechanics of the Euler-Lagrange calculation appear to be in good working order. Secondary effects, such as turbulent-mixing/shock-structure interaction require further study with more test cases. However, it should be noted that suitable experimental data to verify many of these complex flow interactions are not now available. The best one can currently do is compare CFD solutions to SPF-II type analyses.

4. Analyzing large, complex flowfields with any two-phase, finite-rate CFD code is a time consuming process, therefore utilization of all methods which would expedite such analyses should be considered. Analyzing the flowfields with carefully selected subregions and developing parabolized versions of the CFD codes are two such computational aids which should be employed.

References:

1. Y.S. Chen, AIAA Paper 88-0417, Jan. 1988.

2. Y.S. Chen, AIAA Paper 89-0286, Jan. 1989.

3. T.S. Wang and Y.S. Chen, AIAA Paper 90-2494, July 1990.

4. M.D. Sanford, AIAA Paper 91-1789, June 1991.

5. B.E. Launder and D.B. Spalding, Comp. Meth. Appli. Mech.Engr., Vol. 3, pp. 269-289, 1974.

6. Y.S. Chen and R.C. Farmer, AIAA Paper 91-1967, June 1991.

7. Y.S. Chen and R.C. Farmer, 4th Intl. symmp. CFD, Vol.1, 1991.

8. Wang, T.S., Y.S. Chen, and R.C. Farmer, "Numerical Investigation of Transient SSME Fuel Preburner Flowfield with a Pressure Based Reactive CFD Method," 7th SSME CFD Working Group Meeting, MSFC, April 1989.

9. D.J. Carlson & R.F. Hoglund, AIAA J., Vol. 2, Nov. 1964.

10. C.B. Henderson, AIAA J., Vol. 14, p. 707, June 1976.

11. Moylan, B., and P. Sulyma, "Investigation of Gas/Particle Heat Transfer Rates in Solid Rocket Motors," to be presented AIAA Nashville Meeting, June 1992.

12. Smith, S.D., Y.S. Chen, and B.L. Myruski:, "Model Development for Exhaust Plume Effects on Launch Stand Design," March 1991 Progress Report on NAS8-38472, SECA, Inc., Huntsville, AL, April 8, 1991.

13. Dash, S.M., et al, "The JANNAF Standard Plume Flowfield Code Version II (SPF-II), Volume I" Technical Report CR-RD-SS-90-4, Science Applications, Inc., Princeton, NJ, July, 1990.

14. Shuen, J.S., and V. Yang, AIAA Paper-91-0078, January 1991.

15. Freeman, J.A., R.C. Farmer and P.G. Anderson, "Heat Transfer in Rocket Engine Combustion Chambers and Regeneratively Cooled Nozzles," November, 1991 - February, 1992 Progress Report on NAS8-38961, SECA, Inc., Huntsville, AL, February, 1992.